frontiers in Earth Science

ORIGINAL RESEARCH
published: 02 July 2021
doi: 10.3389/feart.2021.685928

# The Driving Forces Underlying Spatiotemporal Lake Extent Changes in the Inner Tibetan Plateau During the Holocene

*Xiangjun Liu*[1,2]*, *David Madsen*[2,3] *and Xiaojian Zhang*[4]

[1]College of Geography and Environmental Science, Northwest Normal University, Lanzhou, China, [2]Salt Lake Institute of Qinghai, Chinese Academy of Sciences, Xining, China, [3]Department of Anthropology, University of Nevada-Reno, Reno, NV, United States, [4]School of Geography and Ocean Science, Nanjing University, Nanjing, China

OPEN ACCESS

**Edited by:**
*Shiyong Yu,*
*Jiangsu Normal University, China*

**Reviewed by:**
*Mingrui Qiang,*
*South China Normal University, China*
*Ulrike Herzschuh,*
*Alfred Wegener Institute Helmholtz Centre for Polar and Marine Research, Germany*
*Jianhui Chen,*
*Lanzhou University, China*

***Correspondence:**
*Xiangjun Liu*
*xiangjunliu@126.com*

**Specialty section:**
*This article was submitted to Quaternary Science, Geomorphology and Paleoenvironment, a section of the journal Frontiers in Earth Science*

**Received:** *26 March 2021*
**Accepted:** *21 June 2021*
**Published:** *02 July 2021*

**Citation:**
*Liu X, Madsen D and Zhang X (2021) The Driving Forces Underlying Spatiotemporal Lake Extent Changes in the Inner Tibetan Plateau During the Holocene. Front. Earth Sci. 9:685928. doi: 10.3389/feart.2021.685928*

The Inner Tibetan Plateau (ITP), the central and western part of the Tibetan Plateau (TP), covers about one-fourth of the entire TP and contains more than 800 endorheic lakes larger than 1 $km^2$. These lakes are important water reservoirs and sensitive to TP climate changes. They regulate regional water circulations, and further influence local ecosystems. Many lakes in ITP are surrounded by conspicuous paleoshorelines indicating much higher past lake levels. Previous studies found that lakes in the western ITP (west of ~86°E) apparently expanded to higher levels than those to the east during the Holocene high lake level stage, however, there is no in-depth study on the reasons for the spatial differences of high lake levels within the ITP. In this study, we first identify Holocene lake level (or lake extent) changes over the ITP by combining published lake level variation data with our reconstruction of Dagze Co lake level variations. We then investigate spatial differences in the magnitude of lake expansions and explore the underlying forces driving these differences using the transient climate evolution of the last 21 ka (TraCE-21ka) and Kiel Climate Model (KCM) simulation results. We find that lakes in the ITP expanded to their highest levels during the early Holocene when the Indian summer monsoon (ISM) greatly intensified. After the mid-Holocene, lake levels fell as a result of the weakening of the ISM. The early Holocene northward shift of the westerly jet and a positive phase of the Atlantic multidecadal oscillation (AMO) resulted in the intensification of southwesterly winds on the southwest TP flank. Concurrently, westerly winds over the TP weakened, causing a differential increase in water vapor transport to the ITP with higher precipitation levels in the southwestern ITP and lower levels to the northeast. These wind-driven differential precipitation levels caused lakes in the southwestern ITP to expand to higher levels than those in the central, northern and northeastern ITP. During the early Holocene, expansion of lakes in the northwestern ITP was enhanced by an increase in glacier melt water besides the increased summer rainfall associated with the intensified ISM.

**Keywords: inner Tibetan plateau, holocene, lake extent changes, lake level variations, paleoshoreline**

## INTRODUCTION

The Tibetan Plateau (TP) is the largest elevated landform on Earth, occupying an area of ~300 × $10^4$ $km^2$ (Zhang et al., 2020). More than ten large Asian rivers originate from the TP, supplying living water for more than one billion people within and surrounding the TP. The TP is rightly regarded as "the water tower of Asia" (Barnett et al., 2005; Immerzeel et al., 2010). Long-term climate changes have reshaped the environment of the TP *via* interactions among the atmosphere, hydrosphere, cryosphere and biosphere (Chen et al., 2020). The variations of environment influenced water budgets over the TP by modulating precipitation and evaporation, which then regulated the size of lakes in the TP and the amount of river discharge flowing out of the TP.

The TP as a whole is situated within the region influenced by the Indo-China monsoons (Conroy and Overpeck, 2011). Using an empirical orthogonal function based regionalization of gridded precipitation values, Conroy and Overpeck (2011) reported that most precipitation in the southwestern TP (region ③ in **Figure 1B**) is related to the Indian summer monsoon (ISM). They also reported that most precipitation in the eastern TP (region ① in **Figure 1B**) is correlated with the East Asian summer monsoon (EASM) which has a significant negative correlation with the western North Pacific summer monsoon (Conroy and Overpeck, 2011). Lai et al. (2021) using a self-organizing map algorithm, analyzed the Global Precipitation Measurement satellite product and ERA5, and determined that the western TP gets most precipitation during the winter and spring seasons that are associated with the westerly jet (blue areas in **Figure 2**). The southwestern TP gains more precipitation during late summer associated with intensity changes in the South Asian High (SAH) and ISM (green areas in **Figure 2**). Eastern TP precipitation is largely related to ISM and anticyclonic circulation over the western North Pacific which peaks during the early summer (yellow areas in **Figure 2**). There are more than 1,000 lakes scattered over the TP, with a total area of ~5 × $10^4$ $km^2$ (Zhang et al., 2019a; Qiao et al., 2019). These lakes are not only sensitive to large scale climate changes, but also have knock-on effects on regional water balances and water vapor circulation (Chen et al., 2020). The changes of lake areas in the TP are considered as direct proxy to illustrate the variations in precipitation (Liu et al., 2021).

The Inner Tibetan Plateau (ITP) locates at the central-western part of the TP (**Figure 1**), it composed of hundreds of endorheic

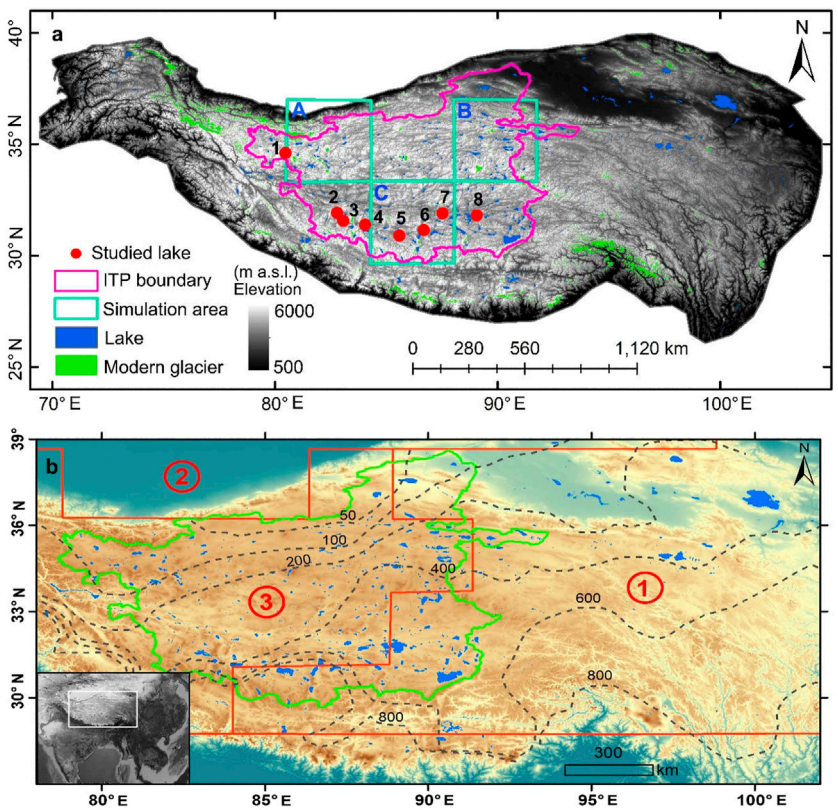


**FIGURE 1 |** Location of the Inner Tibetan Plateau (ITP) within the Tibetan Plateau (TP). Modern closed-basin lakes on the Tibetan Plateau (blue patches). Pink and green lines in **(A)** and **(B)** outline the scope of ITP. The ITP boundary follows Zhang et al. (2013). Red dots in **(A)** are lakes that have reported Holocene lake level variation curves, 1-Longmu Co, 2-Baqan Co, 3-Ngangla Ring Co, 4-Zhari Nam Co, 5-Zabuye Lake, 6-Tangra Yumco, 7-Dagze Co, 8-Seling Co. The cyan squares (marked with A, B and C) in **(A)** are unit-pixels of TraCE-21ka model we used for modeled Holocene precipitation and temperature changes. Red lines in **(B)** outline regional TP precipitation zones proposed by Conroy and Overpeck (2011). Dashed black lines in **(B)** are modern annual total precipitation (mm) contours obtained from a monthly 1900–2014 global gridded precipitation data set (Hudson and Quade, 2013).

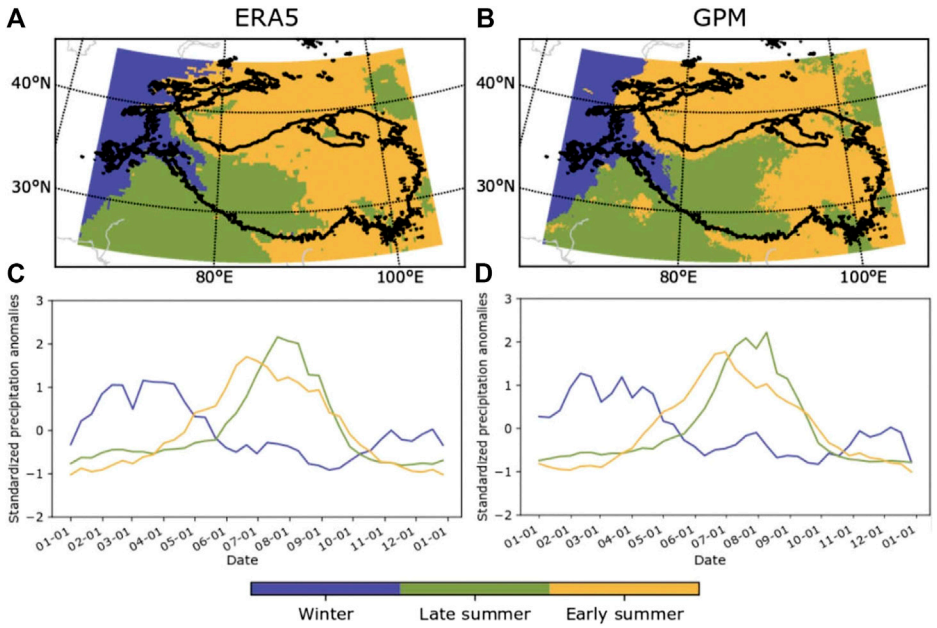


**FIGURE 2 |** Precipitation classification maps of 19-year averaged (2000–2019) seasonal cycles of standardized precipitation from ERA5 **(A)** and Global Precipitation Measurement product **(B)**. Three precipitation regimes of winter precipitation dominant, early summer precipitation dominant, and late summer precipitation dominant are showed with blue, yellow and green colors. **(C)** and **(D)** show the standardized precipitation anomalies of the spatially averaged precipitation for each precipitation regime (modified from Lai et al. (2021); **Figure 3**).

basins that have average elevations of ~4,960 m above sea level (a.s.l.). A map of the spatial extent of the ITP, when laid over spatial TP precipitation classification maps (**Figures 1**, **2**), indicates that the ITP is located primarily within the region influenced by the ISM. At present, the ITP contains about 55% of lakes in the TP, accounting for 66% of the total TP lake area (Li et al., 2019). Lakes in ITP expand and contract in response to dynamic water balance changes between the input water (precipitation, river runoff, and melt water) and evaporation. The recent history of most lakes in the ITP indicates they contracted from 1976–1995, then expanded rapidly after 1996, closely responding to water balance changes related to differences in precipitation, glacier melt water, and evaporation (Zhang et al., 2020). Lakes in the ITP expanded synchronously with an increase in precipitation during the past 30 years (Chen et al., 2020; **Figure 3**). Increased growing season precipitation was the main reason (contributing ~74% of water inflow) causing ITP lakes to expand rapidly during the past 2 decades (Lei et al., 2014; Zhang et al., 2020). Since the mid-1990s, a warm phase of the Atlantic multidecadal oscillation (AMO) induced a wave train of cyclonic and anticyclonic storms during the summer, enhancing the meandering of the westerly jet. This further modulated precipitation over the ITP by changing its position and strength, causing precipitation over the ITP to steadily increase, with ITP lakes expanding in response (Sun et al., 2020). This expansion of lakes in the ITP caused both ecological and social problems, as vast areas of grasslands surrounding the lakes were submerged, the houses of herdsmen were flooded and important infrastructure, such as the Qinghai-Tibetan railway, were threatened by the rising lake waters (Liu et al., 2016a; Yao et al., 2016). As a result of these threats, recent research has focused on lake variations and on predicting future changes (Lei et al., 2014; Yang et al., 2018; Qiao et al., 2019; Zhang et al., 2020), with some studies predicting lakes

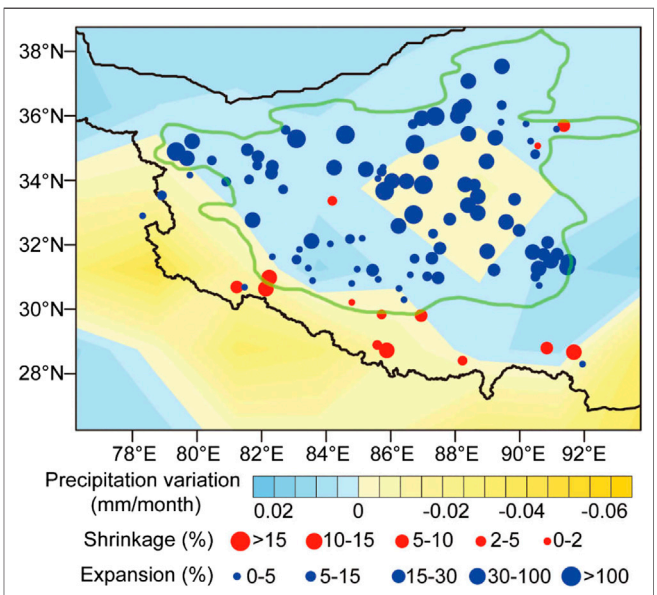


**FIGURE 3 |** Changes in lake area (1976–2010 CE) (solid dots) and precipitation (yellow [–], blue [+]) (1979–2010 CE) on the TP. The green closed line outlines the extent of ITP (modified from Chen et al., 2020; **Figure 5**).

in the TP will continue to expand until at least 2035 (Yang et al., 2018; Zhang et al., 2020).

Most lakes in the ITP have drastically expanded during the past as evidenced by conspicuous regressive shorelines (Hudson and Quade, 2013; Liu et al., 2013). Paleoshoreline dating has been widely used to reconstruct past lake extent changes and paleohumidity, and to quantify paleorainfall on the TP based on paleohydrological modeling (Chen et al., 2020 and references therein). Both paleoshoreline dating results and paleoenvironmental proxies suggest that during the early Holocene (10–8 ka) rainfall substantially increased and lakes in TP significantly expanded in response to intensification of the ISM (Fleitmann et al., 2007; Cai et al., 2012; Chen et al., 2013; Hudson and Quade, 2013; Liu et al., 2013, Liu et al., 2016b; Bird et al., 2014; Hudson et al., 2015; Huth et al., 2015; Shi et al., 2017). However, lakes located in the western TP (west of 86° N) reached higher lake levels than lakes in the eastern TP (east of 86° N), and the magnitude of lake expansion also decreased from west to east (Hudson and Quade, 2013; Liu et al., 2013). This west/east TP lake history asymmetry during the Holocene high lake level stage is thought to have been caused by differential enhancement of the ISM and the EASM (Hudson and Quade, 2013). As the ISM weakened after the mid-Holocene (~6 ka), precipitation decreased and lakes in the central and western TP regressed, most of these lakes are located in the ITP (Bird et al., 2014; Liu et al., 2016b).

In the ITP, the spatial pattern of lake expansions during the Holocene is different from the relatively homogeneous pattern reflected in modern lake expansions (**Figure 3**). Since the relatively even expansion of lakes in ITP in recent decades does not provide a simple analogy for their Holocene expansions, understanding spatial differences during the Holocene high lake level stage and the underlying driving forces can help us better predict future changes. To more comprehensively understand the Holocene lake extent (or lake level) changes in the ITP and to explore the underlying causes, seasonal precipitation changes need to be considered because the ISM and the Westerlies alternatively influenced the ITP during the summer and winter seasons across the Holocene (Zhu et al., 2015). Such needed research has not been conducted. Moreover, the influence of glacier melt water on the lakes in the ITP and their variations during the Holocene is as yet poorly estimated, both qualitatively and quantitatively.

Here, we combine lake extent variation data, lake level variation curves, and modeled glacier coverage map of the last glacial maximum (LGM) with the modeled transient climate evolution of the last 21 ka (referred to as TraCE-21ka) and with the Kiel Climate Model (KCM) simulation. We use this combined data set to summarize the spatial and temporal changes of lake extents (or lake levels) in the ITP during the Holocene and to explore the underlying causes. TraCE-21ka model results have coarse spatial resolution (3.75° × 3.75°), and its simulated data were used to analyze Holocene precipitation and temperature changes over the ITP. The KCM model was used to simulate spatial precipitation and temperature changes over the TP during the early, mid and late Holocene. Although some environmental proxies can reflect moisture or precipitation changes in ITP during the Holocene, they are less useful in describing spatial differences in moisture or precipitation changes in the ITP. Moreover, some proxy-based precipitation reconstructions may be related to climate factors other than precipitation, such as temperature, atmospheric circulation changes, and lake water salinity (Chen et al., 2020). Hence, in this study, we only include pollen-based precipitation reconstruction results within the TP as a reference.

# HOLOCENE LAKE LEVEL VARIATIONS AND HETEROGENOUS EXPANSION OF LAKES IN THE INNER TIBETAN PLATEAU

## Inner Tibetan Plateau Setting and Modern Conditions

The ITP locates at central-western TP with an area of ~70 × $10^4$ $km^2$ (**Figure 1**), it covers more than one fourth of the entire TP with an average elevation of ~4,960 m a.s.l., and it is surrounded by the Tanggula, Gangdise, Kunlun, and Karakorams mountains. Average annual temperature is less than 0°C over the ITP, annual evaporation over lake surfaces is >1,000 mm (Li et al., 2019). Annual precipitation is 500–600 mm in the southern and southeastern ITP, and decreases to less than 100 mm in the northwestern ITP (**Figure 1B**). At present, there are about 820 endorheic lakes larger than 1 $km^2$ lie in the ITP (Zhang et al., 2019a). The ITP lies in the transition zone between the Westerlies and the Indian monsoon, hence lakes in ITP are sensitive to climate changes associated with Westerlies and the ISM interactions (Yao et al., 2012; Li et al., 2019).

## Previous Research on Inner Tibetan Plateau Holocene Lake Level Variations

Paleoshorelines provide evidence of past lake levels and can be dated to reconstruct lake level variation histories and to investigate past moisture changes over lake drainage basins (Quade and Broecker, 2009). Paleoshorelines surrounding lakes in the ITP are distinct and well preserved due to limited human modifications (**Supplementary Figure S1**). During the past 20 years, increasing numbers of paleoshorelines in the ITP have been dated as improvements in dating precision and reductions in age uncertainties of non-radiocarbon dating methods have progressed. These new age estimates, derived primarily from Optically Stimulated Luminescence (OSL) methods, have been used in combination with $^{14}C$ ages to define lake level fluctuation histories (Lee et al., 2009; Li et al., 2009; Chen et al., 2013; Rades et al., 2013; Ahlborn et al., 2015; Huth et al., 2015; Hudson et al., 2015; Liu et al., 2016b; Shi et al., 2017; Alivernini et al., 2018; Hou et al., 2020; Jonell et al., 2020). Although high-stand paleoshoreline ages for many lakes have been reported, Holocene lake level variations for only a few have been described, including Seling Co (Shi et al., 2017; Hou et al., 2021), Baqan Co (Huth et al., 2015), Tangra Yumco

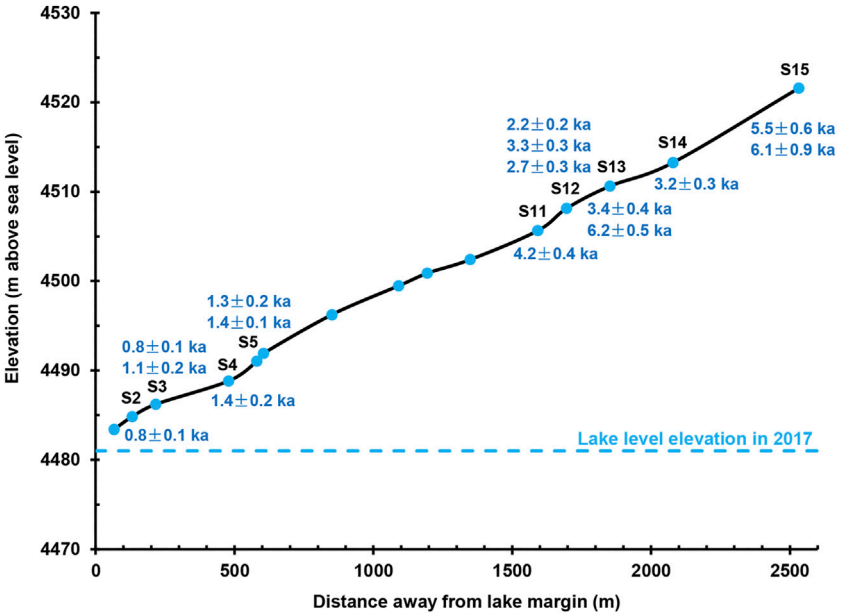


**FIGURE 4 |** Elevations plotted against the distances from the lake margin for corresponding paleoshorelines in Dagze Co. The associated OSL ages are shown above or below the corresponding paleoshorelines. The locations of OSL dating samples were marked in **Supplementary Figure S2**, and the details of OSL ages were shown in **Table S1**.

(Ahlborn et al., 2015), Zhari Nam Co (Chen et al., 2013), Ngangla Ring Co (Hudson et al., 2015), Longmu Co (Liu et al., 2016b), Zabye Lake (Alivernini et al., 2018), and Dagze Co (reported below). Seven out of these eight lakes are located in the southern ITP, with only Longmu Co being located in the western ITP (**Figure 1A**). Several other lakes in the central and northern ITP also have reported paleoshorelines or lacustrine sediment ages, but these ages are very limited in numbers (only very few highstand lacustrine sediments or paleoshorelines were dated) and/or only indicate a highstand stage, and not enough to be used to reconstruct lake level variation histories (Long et al., 2012; Ma et al., 2012; Pan et al., 2012; Hou et al., 2020).

## Dagze Co Holocene Lake Level Variations

We previously reported OSL ages of ~22.7 and 6.1–5.5 ka for the late glacial and Holocene highstands of Dagze Co, respectively (Liu et al., 2020). Here, we add to these other lake records by presenting a newly reconstructed Holocene lake level fluctuation curve for Dagze Co, based on OSL dating of paleoshorelines (**Supplementary Figure S2**).

Dagze Co, with a modern lake surface elevation of 4,480 m a.s.l., is located in the southern ITP (31.82°–31.98°N, 87.36°–87.65°E) (see Liu et al. (2020) for setting and modern climate descriptions). We identified and mapped 15 paleoshorelines surrounding the now brackish lake. The highest paleoshoreline we identified, S15, is ~41.6 m above the modern lake level, and was formed during the mid-Holocene (**Figure 4**). We obtained OSL age estimates for eight other paleoshorlines which appear to have formed during brief stillstands as the lake regressed from this Holocene high (see Liu et al. (2020) for field and laboratory methods). Dagze Co would have overflowed to the west into lower basins when it reached the highest level at S15 as evidenced by a remnant channel connecting Dagze Co with the western basins (Liu et al., 2020). The dividing crest between Dagze Co and the western basins is approximately the same elevation as paleoshoreline S15. Hence, the lake level would maintain approximately the same height as paleoshoreline S15 or slightly higher during the early Holocene ISM intensification stage when several other lakes in ITP experienced their highest Holocene lake levels (Liu et al., 2016b; Liu et al., 2020). The Holocene lake level variation curve for Dagze Co was then reconstructed based on the OSL ages of these nine paleoshorelines (**Figure 4**).

## Holocene Lake Level Variations in the Inner Tibetan Plateau

Longmu Co lake levels started to rise following the last deglacial, with the lake reaching its peak during the earliest Holocene (**Figure 5**). The lake level was dropped abruptly during the Young Dryas (YD) cold interval, and then maintained in a secondary high level during the early Holocene (10–8 ka), but lake levels dropped abruptly again at ~7.2 ka (**Figure 5**). At the seven other ITP lakes the highest lake levels all occurred between 10 and 8 ka (**Figure 5**), consistent with lacustrine and stalagmite records indicating summer season rainfall substantially increased during the early Holocene in the region influenced by the ISM (Fleitmann et al., 2007; Bird et al., 2014). The levels of Baqan Co, Tangra Yumco, Zhari Nam Co, and Zabye Lake initially began to decline between 8and 7 ka, while the lake levels of Dagze Co and Ngangla Ring Co began to decline at 5.5–6 ka (**Figure 5**),

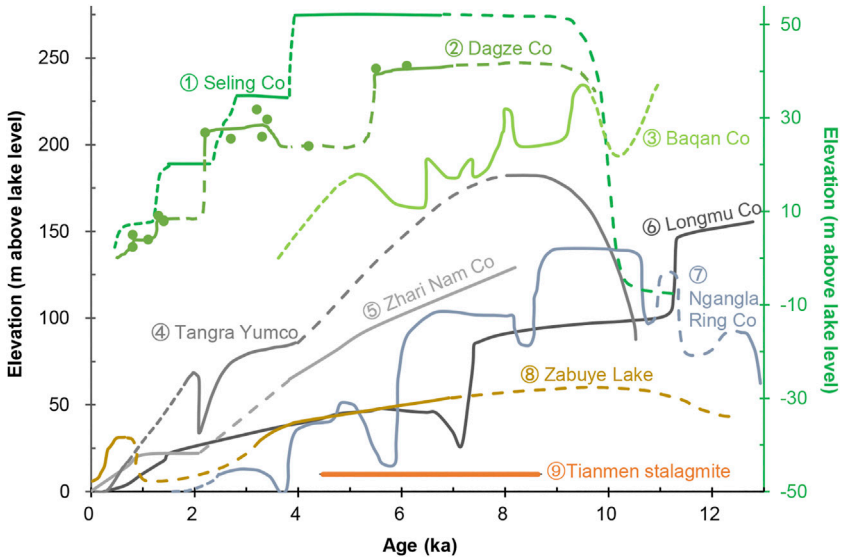


**FIGURE 5 |** Holocene lake level variations in the ITP. ① Seling Co (Shi et al., 2017), ② Dagze Co (our study), ③ Baqan Co (Huth et al., 2015), ④ Tangra Yumco (Ahlborn et al., 2015); ⑤ Zhari Nam Co (Chen et al., 2013); ⑥ Longmu Co (Liu et al., 2016b); ⑦ Ngangla Ring Co (Hudson et al., 2015); ⑧ Zabuye Lake (Alivernini et al., 2018). ⑨ is the growth period of the Tianmen stalagmite (Cai et al., 2012), near Nam Co in the eastern ITP. Note: the three green lines correspond to the right ordinate axis marked with green color.

corresponding to the initial weakening of the ISM during the mid-Holocene (Fleitmann et al., 2007; Bird et al., 2014; Cai et al., 2012). In contrast, the lake levels of Seling Co and Zabuye Lake remained steady or declined only slightly before 4 ka, regressing rapidly in a stepwise fashion after 4 ka (**Figure 5**). A stalagmite adjacent to Nam Co also stopped growing after ~4.2 ka when the ISM weakened and the climate became more arid (**Figure 5**; Cai et al., 2012). As we discuss below, the reasons for these divergent initial lake regression times are complex, but may include differences in precipitation in each lake basin, differences in glacier melt water supply, and difference in precipitation related to local water vapor recirculation. In addition, a recent study proposed that the abrupt lake level drops may related to the disintegration of ancient mega-lakes that were formed when the available water over the TP was plenty during the early Holocene (Jonell et al., 2020).

## Spatial Lake Expansions in Inner Tibetan Plateau During the Holocene Highest Lake-Level Stage

While paleoshorelines are a useful indicator of past climate changes, they can be difficult to interpret since their formation can be influenced by terrain differences in individual watersheds and thus their association with paleo-precipitation changes may not be sufficiently direct. To address this issue, we use lake area ratios (*Aw*), the ratio of summed lake or paleolake areas to the total basin area for each basin system, to make climatic inferences from grouped lake histories. *Aw* reduces the influence of watershed differences on lake histories and is more directly related to annual precipitation (Hudson and Quade, 2013). The analysis showed that differing evaporation rates in different lake and differing lake area to lake volume ratios were not the main parameters that determine the paleolake expansion patterns during the Holocene high lake level stage (Hudson and Quade, 2013). Melt water was also not a dominant factor that caused lakes in the TP expanded synchronously during the Holocene high lake level stage because glacier melting is more related to local climate conditions and lakes with and without glaciers in their catchments expanded in a similar pattern (Hudson and Quade, 2013). Hence, the ratio of paleo-*Aw* to modern *Aw* mainly represents the expansion of a lake in response to past increased precipitation (Liu et al., 2019). Here we use modern lake areas, largest Holocene lake areas and watershed areas reported by Hudson and Quade (2013) for lakes in the ITP. We then calculate paleo-*Aw*s, modern *Aw*s and their ratios for each lake to investigate spatial differences in lake transgression/regression patterns.

We investigated the spatial distributions of modern *Aw* in response to modern precipitation, which decreases from the southern and southeastern ITP to the northwestern ITP, to explore if lakes in more arid regions require larger basins to maintain lakes as the same size as those in relatively wet regions. That is, do lakes in arid regions have smaller *Aw*s when compared with those located in wet regions? Result demonstrates that lakes in the ITP have relative uniform *Aw* values (**Figure 6**), with no significant spatial variations. This suggests that the basin sizes of lakes in different precipitation zones do not dictate how the lakes respond to the varied precipitation amount. This may be because lakes in different precipitation zones have salinity differences which influence surface evaporation. Lakes in arid regions have relative high salinity which reduces lake surface evaporation because salts absorb atmospheric water vapors (Li et al., 1992),

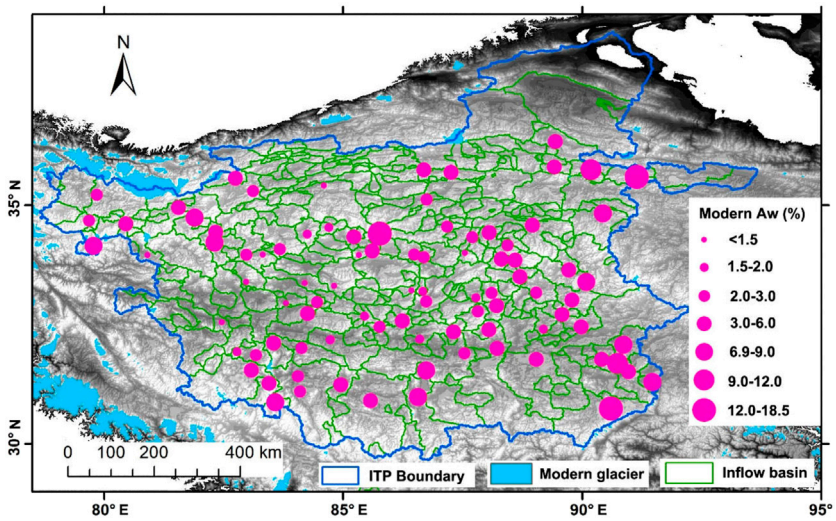


**FIGURE 6 |** Modern *Aw* (ratios) of lake areas to catchment areas. The blue line is the boundary of the ITP. The blue patches are modern glaciers. The green lines are lake catchment boundaries for ITP lakes. Pink dots represent the modern *Aw*.

while lakes in wet regions have relatively low salinity which enhances evaporation.

We also compared the size and distribution of modern ITP lakes to lakes at their highest Holocene levels (**Figure 7**). At present, large lakes (>500 $km^2$) are primarily distributed along the southern and eastern margins of the ITP, while lakes in the central and northwestern ITP are mostly smaller than 400 $km^2$ (**Figure 7A**). Large modern lakes are distributed in the regions where annual precipitation is relatively high (**Figure 1B**). During the early Holocene highstands, large lakes (>500 $km^2$) were found along the western, southern, and eastern margin of ITP, while those smaller than 500 $km^2$ were mostly distributed in the central and northern ITP (**Figure 7B**). The spatial lake size distribution pattern during the early Holocene highstand was generally similar to the modern lake size distribution pattern except for several lakes in the western ITP. This suggests large lakes expanded more in terms of surface areas. While small lakes also expanded, their surface areas remained smaller, in relative terms, than the large lakes (**Figure 7B**). From **Figures 6**, **7**, we deduce that precipitation instead of lake basin size was an important factor influencing the magnitude of lake expansion during the Holocene highstands. Hudson and Quade (2013) also indicate that glacial melt water differences, varied evaporation rates and differing lake area/volume relationships were not the dominant forces which controlled Holocene lake expansions in the TP. They concluded that the patterns of lake expansions in different parts of the ITP is best explained by regional precipitation differences.

We also explored spatial variations in lake level heights and *Paleo-Aw* to modern *Aw* ratios in the ITP during the highest Holocene lake level stage. **Figure 8A** shows that many lakes in the western and southwestern ITP had lake levels more than 80 m higher than at present. Lake levels were 15–40 m higher than present in the central ITP and less than 15 m higher in the northeastern ITP (**Figure 8A**). The ratios of paleo-*Aw* to modern *Aw* have the same spatial trend, with the ratios of paleo-*Aw* to modern *Aw* gradually decreasing in a southwest-northeast direction (**Figure 8B**). Using the concept Hudson and Quade (2013) proposed, this spatial pattern in paleo-*Aw* to modern *Aw* ratios suggests that the increase in precipitation associated with the enhanced ISM may have extended into the ITP from the southwestern TP, with the southwestern ITP getting more rainfall because the atmospheric water vapors first reached there and formed precipitation. Additionally, glaciers over the TP advanced during the LGM (Yan et al., 2018), might providing increased glacier melt water supplies to lower elevation lakes during the last deglacial and Holocene, contributing to rising lake levels. Glaciers expanded markedly in the western ITP and along the southern boundary of the ITP during the LGM (**Figure 8**), supplying additional melt water to lakes in the western and southern ITP. In the western ITP, Longmu Co obtained plenty of melt water supply since last deglacial, its lake level reached the peak at the end of the Bølling warm period and the onset of Holocene (Liu et al., 2016b). Lake levels then dropped abruptly during the Younger Dryas and at ~7.2 ka (**Figure 5**). Li et al. (2021) investigated the authigenic carbonate $\delta^{18}O$ of a glacier fed lake in the western ITP and quantitatively estimated glacier melt water variations during the Holocene based on a hydrological balance model incorporating $\delta^{18}O$. They found that glaciers in the western Kunlun Mountain melted substantially during the early Holocene, but melted only slightly during the late Holocene. Hou (2019) proposed that the Chongce glacier (western TP) may have completely melted during the early Holocene high temperature stage, but redeveloped during the mid and late Holocene. This all suggests that lake level variations in the western ITP were substantially influenced by glacier melt water during the deglacial and early Holocene. Lakes in the southern ITP, on the other hand, rose steadily following the earliest Holocene, reaching their highest levels between 10 and 8 ka (**Figure 5**), as they were synchronized with the

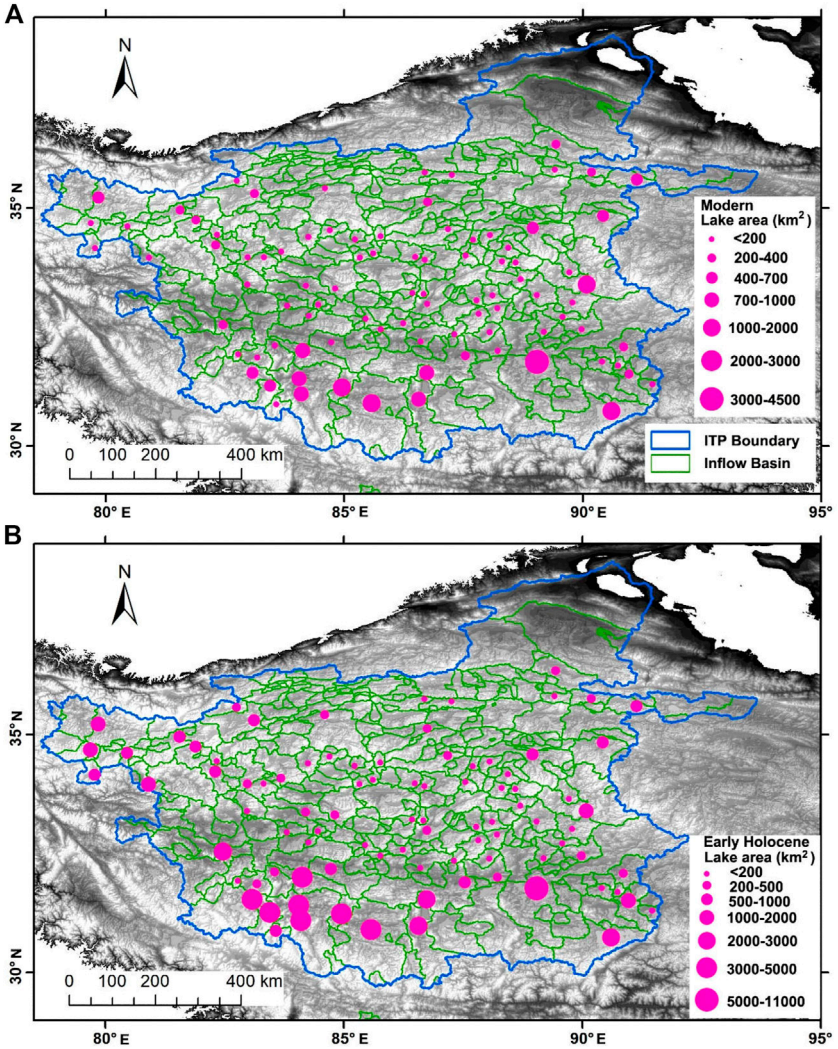


**FIGURE 7 |** Lakes and their sizes at **(A)** modern and **(B)** early Holocene for lakes in ITP. Blue line outlines the boundary of ITP. Green lines outline lake catchment boundary for lakes in ITP. Pink dots show lake sizes.

intensification of the ISM (Fleitmann et al., 2007). In addition, lakes located at the southern ITP west of 86° E expanded substantially more than lakes to the east (**Figure 8B**). Because the Holocene lake level variations in southern ITP are synchronous with the ISM variations, we then speculate that lakes in the southern ITP are primarily controlled by the ISM, and that glacier melt water only plays a secondary role in lake level variations.

## CLIMATE MODEL SIMULATIONS

### Seasonal Precipitation and Temperature Changes Based on the TraCE-21ka Model

The TraCE-21ka climate model provides estimates of seasonal precipitation and temperature changes for the past 21 ka. The TraCE-21ka simulation employs realistic external forcing, including orbital insolation, greenhouse gases, ice sheets, and freshwater fluxes (Liu et al., 2009). The model consists of four coupled components (atmospheric-model, oceanic-model, land-model, and sea ice-model) (Yan et al., 2020). The spatial resolution of the TraCE-21ka simulation is 3.75° × 3.75° in the ITP. We use these simulated seasonal precipitation and temperature changes to explore why lakes in the ITP expanded during the early Holocene, but regressed asynchronously following the mid-Holocene. We select three units that cover the northwest, northeast, and south parts of ITP, and then average the precipitation and temperature data of these three units to obtain the corresponding data for the ITP as a whole (**Figure 1A**).

The TraCE-21ka simulated seasonal precipitation and temperature changes in the ITP are shown in **Figure 9**. Spring (from March to May, MAM) precipitation is relatively stable, with no long-term trend in variation, but fluctuates frequently throughout the Holocene (**Figure 9A**). Summer precipitation (from June to August, JJA) is relatively high between 12 and 9 ka,

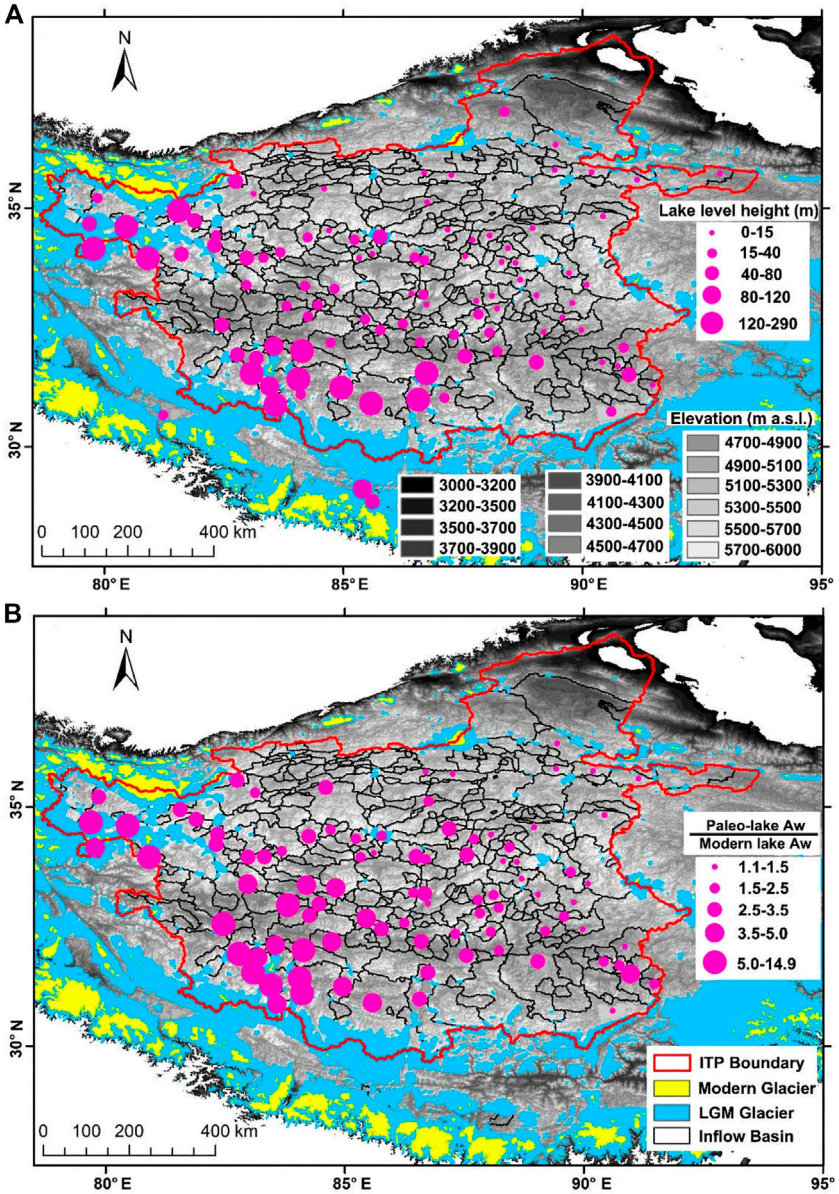


**FIGURE 8 |** Highest early Holocene lake levels above present lake surfaces **(A)** and Paleolake *Aw* versus modern *Aw* ratios of the highest Holocene lake level stage **(B)** for lakes in the ITP. The red line is the ITP boundary. The black lines are lake catchment boundaries. The colored patches show glacier extents during the LGM (blue) and at present (yellow) (Yan et al., 2018). The pink dots in **(A)** show lake level heights, and in **(B)** show the ratios of Paleolake *Aw* to modern *Aw*.

slightly decreases from 8–6 ka, substantially declines from 6–4 ka, and is maintained at lower values, but with substantial fluctuations during the past 4 ka (**Figure 9A**). Autumn precipitation (from September to November, SON) increases from 12–10 ka, stays relatively high with substantial fluctuations between 10 and 6 ka, then decreases after 6 ka (**Figure 9A**). Winter precipitation (from December to February, DJF) continuously increases across the Holocene (**Figure 9A**). Annual precipitation and net annual precipitation (precipitation minus evaporation, abbreviated as P-E) co-varies across the Holocene, they increase from 12–10 ka, are maintained at high values between 10 and 6 ka, decline from 6–4 ka, and slightly decrease during the last 4 ka (**Figure 9A**). Net annual precipitation change represents effective moisture changes, and further reflects basin-wide water balance variations. Lake level variations in the ITP across the Holocene are similar to net annual precipitation changes (**Figures 5**, **9A**). They also co-vary with annual precipitation, JJA precipitation and SON precipitation, suggesting that summer and autumn precipitation were important for annual precipitation changes and were the dominant influence on Holocene lake level variations in the ITP.

During the Holocene, modeled winter, spring, and autumn average temperatures are below zero centigrade and only summer

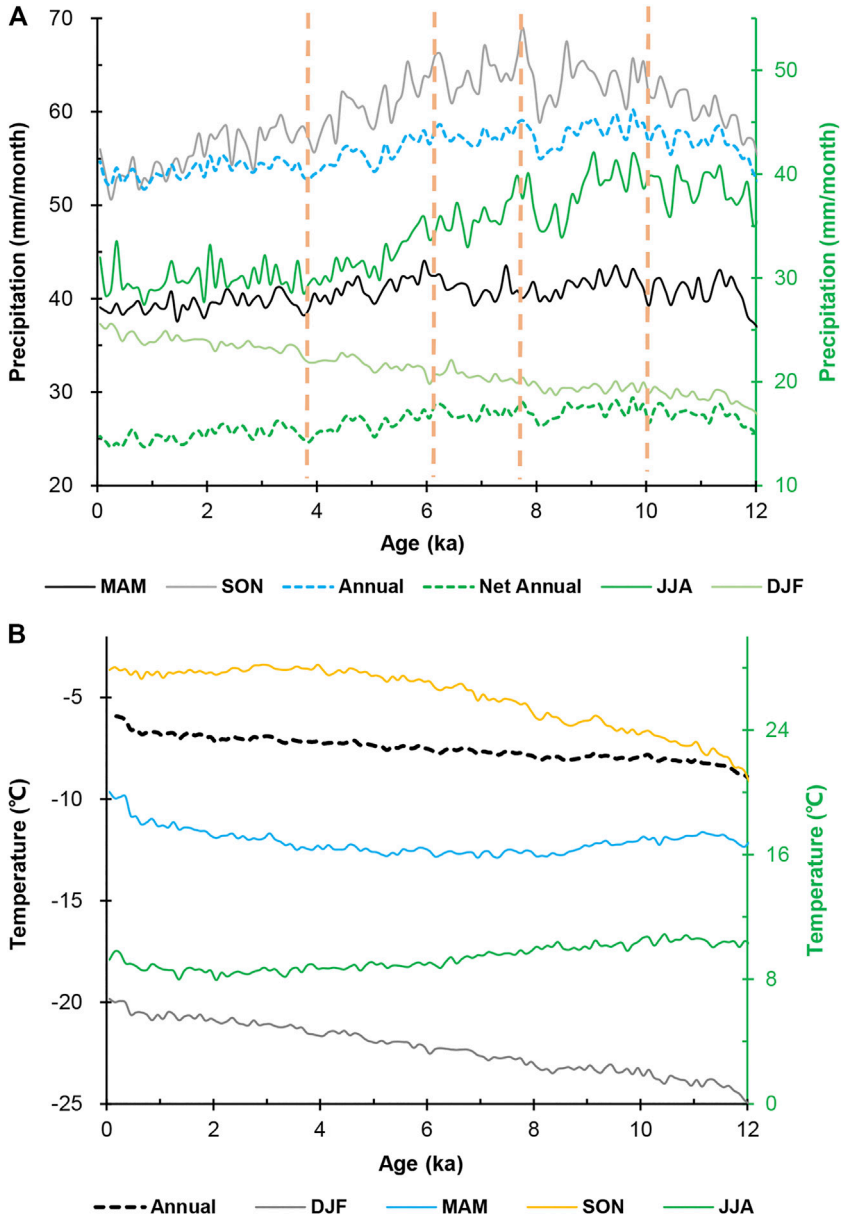


**FIGURE 9 | (A)** TraCE-21ka modeled annual precipitation, seasonal precipitation (MAM, JJA, SON, DJF) and net annual precipitation (P-E) over the ITP, **(B)** TraCE-21ka modeled annual and seasonal temperature (MAM, JJA, SON, DJF) over the ITP. Note: three green lines in **(A)** and one in **(B)** correspond to the right ordinate axis marked with green color.

temperatures are above zero (**Figure 9B**). However, modeled summer temperatures decline following the early Holocene (**Figure 9B**). Since high summer temperatures may enhance lake surface evaporation and inhibit lake expansion on the one hand, on the other hand, high summer temperatures may enhance regional water vapor recirculation over the ITP. At present, the precipitation recycle ratio over the TP during the summer is ~23% (Zhao and Zhou, 2021), and large lakes in the TP reshape regional precipitation patterns and also influence precipitation amounts adjacent and downwind of them (Dai et al., 2020a; Dai et al., 2020b). During the early Holocene, enlarged lakes, and elevated summer temperatures would conducive to precipitation recycling within the ITP that helped to maintain lakes in high lake levels.

## Holocene Spatial Precipitation Changes in the Inner Tibetan Plateau Based on the Kiel Climate Model

In order to more comprehensively understand why lakes in the southwestern ITP expanded more than lakes in the northern and northeastern ITP during the Holocene highstand, we simulated

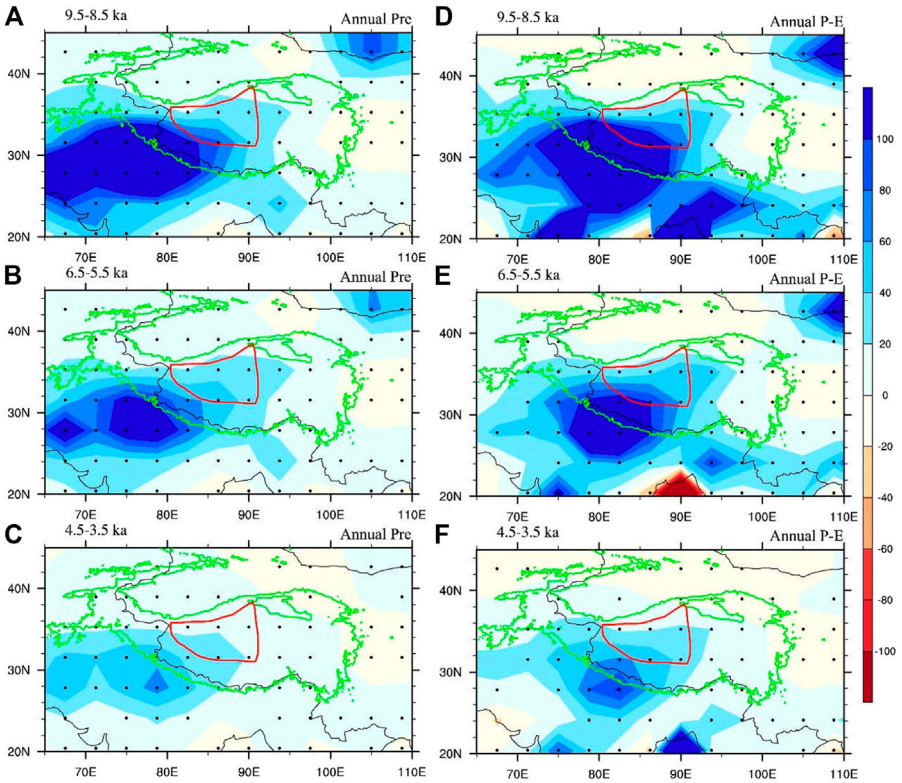


**FIGURE 10 |** Percentage changes of annual precipitation during the early Holocene **(A)**, mid-Holocene **(B)**, and late Holocene **(C)** relative to the past 1 ka over the TP and surrounding areas based on Kiel Climate Model (KCM) simulations. Corresponding percentage changes of annual P-E are shows in **(D–F)**. The red closed line outlines approximate extent of the ITP.

seasonal, annual, and net precipitation (P-E) changes for the early Holocene (9.5–8.5 ka), mid-Holocene (6.5–5.5 ka), and late Holocene (4.5–3.5 ka) relative to the last 1 ka over the TP and its adjacent areas using the KCM. The KCM model is a non-flux-corrected coupled general circulation model. This Holocene climate simulation holds Greenhouse Gas concentrations constant at pre-industrial levels, but adjusts orbital precession from 9.5–0 ka with a ten-fold acceleration scheme (Jin et al., 2014; see Park et al. (2009) for a detailed description of the KCM model).

KCM simulation results show that annual precipitation significantly increases over the southwestern TP during the early Holocene (9.5–8.5 ka), and that the relative amount of precipitation increase lessens along a southwest-northeast route toward the inner TP (**Figure 10A**). Annual P-E has the same modeled trends in variation as that of annual precipitation (**Figure 10D**), suggesting that the increase in precipitation is the dominant controlling factor for water balance changes in the ITP. KCM modeled spatial percentage changes in annual precipitation and annual P-E can explain why lakes in southwestern ITP expanded more dramatically, with a decreasing magnitude of expansion towards the northern and northeastern ITP (**Figure 8**). Modeled precipitation and P-E over the ITP decrease throughout the mid- and late Holocene (**Figure 10**), consistent with the shrinkage of lakes after the mid-Holocene. Regions with significant precipitation increases in TP generally overlap with regions influenced by the ISM as Lai et al. (2021) outlined using a self-organizing map algorithm to analyze the Global Precipitation Measurement satellite product and ERA5 (**Figure 2**). This confirms a proposal by Conroy and Overpeck (2011) that the early Holocene amplified ISM resulted in a monsoon precipitation increase rather than a northward shift in the monsoon boundary. Hudson and Quade (2013) also suggested that the areas influenced by the modern ISM and EASM persisted throughout the Holocene, with the ISM-influenced western TP gaining more rainfall than the EASM controlled eastern TP during the early Holocene high lake level stage.

We also investigated seasonal precipitation and P-E changes over the ITP during the Holocene and their potential contributions to lake level variations. Modeled spring (MAM) precipitation substantially increases during the early Holocene, but this increase lessens from the southwestern to northeastern ITP (**Supplementary Figure S3A**). Modeled spring P-E suggests early Holocene effective moisture mainly increases across the southern ITP, while the P-E over the northern ITP increases only slightly (**Supplementary Figure S3D**). Spring precipitation and P-E decline during the mid-Holocene, with no evident changes

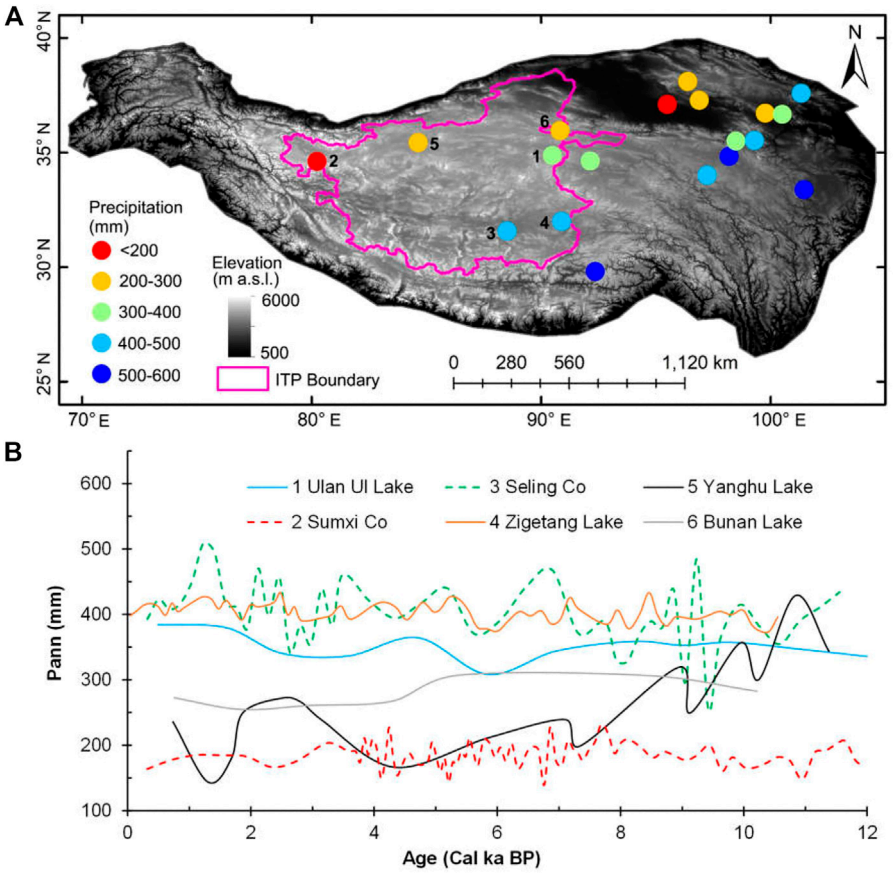


**FIGURE 11 | (A)** Pollen-based reconstruction of annual precipitation in TP during the last 2 ka, the pink line outlines the area of ITP. **(B)** Pollen-based reconstruction of Holocene annual precipitation for six lakes in ITP. The data was obtained from Herzschuh et al. (2019).

from the mid- to late Holocene (**Supplementary Figure S3**). Summer (JJA) precipitation significantly increases over the western TP during the early Holocene, and decreases after the mid-Holocene (**Supplementary Figures S4A–C**). Summer P-E over the ITP substantially increases during the early Holocene, slightly decreases during the mid-Holocene, and then rapidly declines during the early stages of the late Holocene (**Supplementary Figures S4D–F**). Modeled autumn (SON) precipitation increases in the southwestern TP throughout the Holocene, but the percentage increases are highest during the early Holocene, decreasing slightly after the mid-Holocene (**Supplementary Figures S5A–C**). Modeled autumn P-E indicates that effective moisture in the ITP increases during the early and mid-Holocene, but the western and northern ITP becomes dry following the early stage of the late Holocene (**Supplementary Figures S5D–F**). Winter (DJF) precipitation and P-E change only a little in the ITP through the Holocene (**Supplementary Figure S6**). A synthesis of the seasonal precipitation and P-E changes in the ITP during early, mid and late Holocene, suggests that the increased precipitation during the spring, summer, and autumn seasons contributed to the marked early Holocene lake expansions in the ITP. According to the modern observations, the increased spring precipitation was due mainly to moisture input from the Eurasian continent (Zhang et al., 2019b; Li et al., 2019). Increased rainfall during the summer season was mostly correlated with intensification of the ISM, while increased autumn precipitation came partially from the prolonged seasonal influence of the ISM and partially from enhanced water vapor recycling over the ITP (Li et al., 2019; Zhao and Zhou, 2021). After the mid-Holocene, the summer and autumn percentage of annual precipitation declined, causing lakes in the ITP to regress as a consequence (**Supplementary Figures S4, S5**). **Figure 8** illustrates that the expansion of lakes in the southwestern ITP was much greater than lakes located in the central, northern, and northeastern ITP. This spatial contrast in lake expansion is consistent with spatial differences in annual precipitation and net annual P-E changes during the early Holocene (**Figure 10**), suggesting that an increasing spatial differentiation in annual precipitation may have been an important driver of differential lake transgressions in the ITP. The nearly synchronous variations of percentage changes in annual

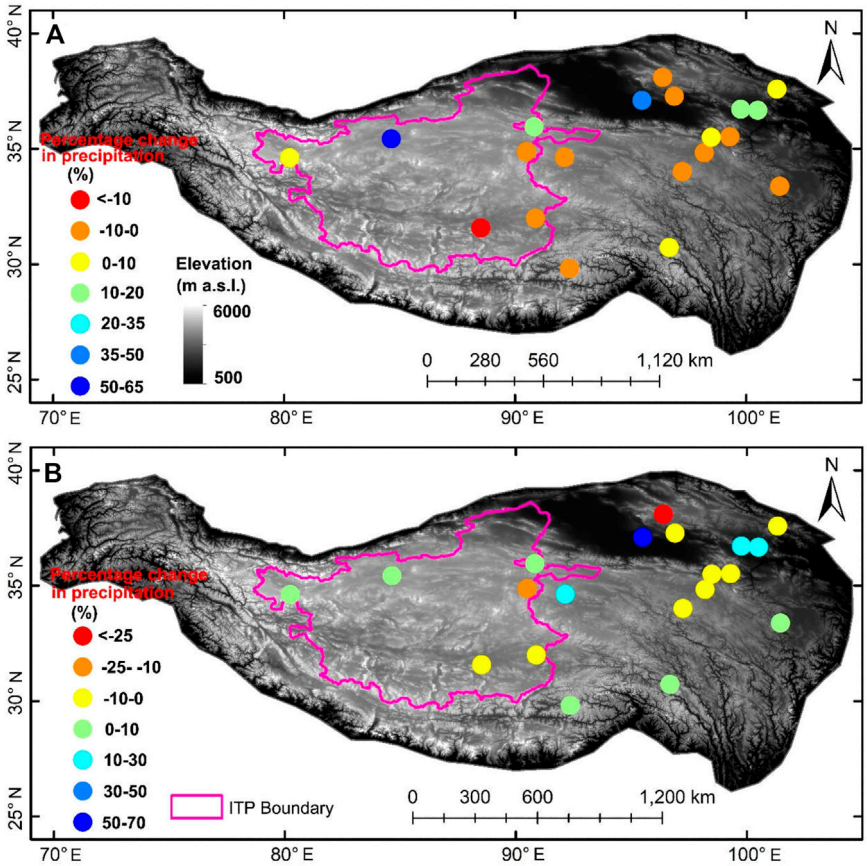


**FIGURE 12 |** Pollen-based reconstruction of percentage precipitation changes in TP during the early Holocene [12–8 ka] **(A)** and mid-Holocene [7–4 ka] **(B)** relative to the past 2 ka, respectively. The pink line outlines the area of ITP. The data was obtained from Herzschuh et al. (2019).

precipitation and net annual P-E suggest that precipitation was the dominant component influencing effective moisture changes in the ITP during the Holocene (**Figure 10**).

## POLLEN-BASED HOLOCENE PRECIPITATION RECONSTRUCTIONS IN INNER TIBETAN PLATEAU

Several researches reported that the climate in southern and western TP were wettest during the early Holocene (from 10–7.5 ka), but became dry since ~7.5 ka (Gasse et al., 1991; Bird et al., 2014; Chen et al., 2020; Zhang et al., 2021). These researches are consistent with paleoshoreline dating results that the highest lake level for most lakes in central, southern, and western TP occurred during the early Holocene. However, these proxies cannot provide valuable information about changes in precipitation amount and its spatial variations during the Holocene over the TP.

Recently, Herzschuh et al. (2019) quantitatively reconstructed changes of annual precipitation in China during the Holocene by using fossil pollen datasets. They assume that vegetation types and pollen composition are mainly determined by precipitation. We extract the relevant data covering the TP from their datasets to compare the results with our own. There are six lakes within the ITP (**Figure 11A**). Pollen-based result shows precipitation of the last 2 ka in the southeastern ITP was 400–500 mm, and decreased to 200–300 mm in northern ITP and to <200 mm in northwestern ITP (**Figure 11A**). The magnitude and spatial distribution of the pollen constructed precipitation are consistent with modern precipitation changes across the ITP (**Figure 1B**). The pollen reconstructed precipitation in Yanghu Lake and Bunan Lake in northern ITP were high during the early Holocene, but decreased since mid-Holocene (**Figure 11B**). However, temporal trends in the reconstructed precipitation of the Ulan Ul Lake, Seling Co, Sumxi Co, and Zigetang Lake are not obvious, but with centennial to millennial fluctuations (**Figure 11B**). We further analyzed percentage precipitation changes in the early (12–8 ka) and mid-Holocene (7–4 ka) relative to the last 2 ka for lakes over TP. During the early Holocene (12–8 ka), precipitation in the Yanghu Lake and Bunan Lake in northern ITP increased, while over the other four lakes decreased (**Figure 12A**). During the mid-Holocene (7–4 ka), three lakes in northern ITP show slight increase in precipitation, while the other three lakes in central and southern

ITP show slight decrease in precipitation (**Figure 12B**). Generally, precipitation over TP is higher during the mid-Holocene than the early Holocene (**Figure 12**).

Pollen-based precipitation in southeastern ITP during the early and mid-Holocene was lower than the late Holocene (last 2 ka) (**Figure 12**). However, the KCM simulated results show the precipitation in southeastern ITP was higher during the early and mid-Holocene than the late Holocene (**Figure 10**). Furthermore, lakes in southeastern ITP also expanded to some extent during the early Holocene (**Figure 8**). Pollen-based precipitation in northwestern ITP during the early Holocene was also lower than the late Holocene (**Figure 12**), in contrast to KCM simulated increase in precipitation and drastic expansions of lakes (Longmu Co and Sumxi Co). Lacks of reconstructed precipitation record in central and southwestern ITP where lakes expanded more drastic during the early Holocene, which limit our ability to estimate the contributions of precipitation and melt water to the expansions of lakes in these regions. The discrepancy between pollen-based precipitation changes and KCM model results in ITP, and the expansion of lakes may in one hand due to the amounts of glacier melt water are hard to be estimated that supply the lakes, and in another hand to that pollen assemblages may contain certain portions of long distance transported pollens which introduce uncertainties in the precipitation reconstructions (Zhao et al., 2021). In addition, the response of ecosystem (soil moisture and tree cover) to precipitation variations can lag for several thousand years due to the impacts of winter warming (Cheng et al., 2021).

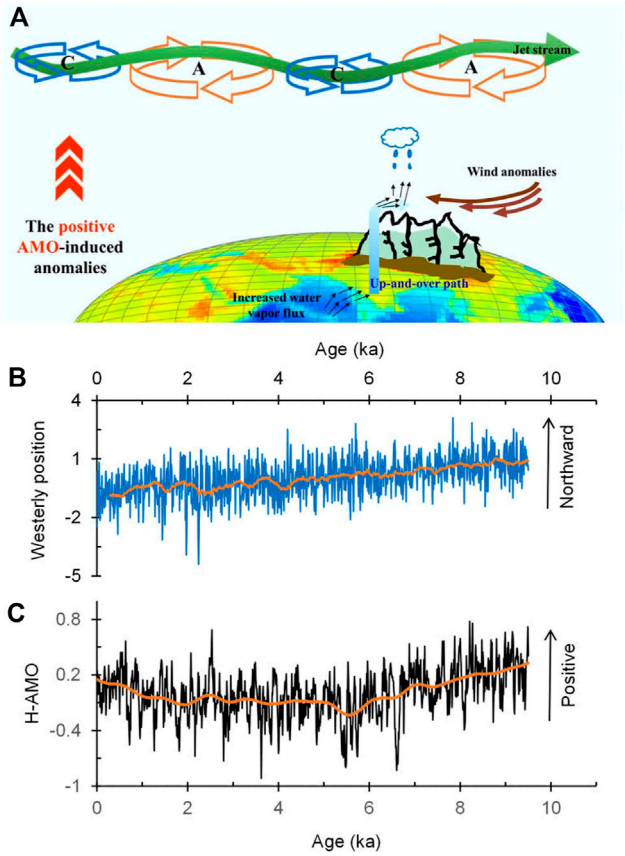


**FIGURE 13 | (A)** Schematic cartoon diagram of Atlantic multidecadal oscillation (AMO) influence on variability in summer precipitation over the ITP (Sun et al., 2020, **Figure 11**). **(B)** Northern Hemisphere westerly jet position changes during the Holocene (Zhang and Jin, 2018). **(C)** Holocene evolution of the Atlantic multidecadal oscillation estimated from a KCM simulation (Zhang et al., 2016).

## THE REASONS FOR SPATIAL DIFFERENCES OF PRECIPITATION IN INNER TIBETAN PLATEAU DURING THE EARLY AND MID HOLOCENE

A number of recent studies indicate the ITP lies in an area where precipitation is most closely linked to the ISM (Conroy and Overpeck, 2011; Lai et al., 2021). An increase in modern ITP precipitation is correlated with interdecadal time scale changes of the AMO and related changes in the strength of the subtropical westerly jet stream near and over the TP (Sun et al., 2020). Liu et al. (2021) reported that intimate correlation existed between the moisture budget in the TP and the AMO as well as interdecadal Pacific oscillation (IPO). The IPO can exert impact on the TP moisture budget by affecting the westerly jet stream (Liu et al., 2021). The AMO has been regarded as the key factor influencing summer rainfall over the ITP (Sun et al., 2020). First, the AMO warm phase induces an anomalous summer cyclonic and anticyclonic wave train over Eurasia, causing the westerly jet to weaken and shift northward (Sun et al., 2020). Second, while the westerly jet over the TP weakens, the westerly jet to its west remains strong, causing enhanced air convergence over the TP (Sun et al., 2020; Liu et al., 2021). Water vapor then intrudes into the ITP through an "up-and-over" moisture transport pattern (Dong et al., 2016). Third, the weaker westerly winds over the TP in turn weakens water vapor transport at increasing distances from its eastern boundary (Liu et al., 2021). A strong cyclone west of the ITP concurrently enhances southwestern winds and convection over the India subcontinent, promoting water vapor transport from the Arabian Sea (**Figure 13A**). During the past 3 decades, lake expansions over the ITP are, as a result, attributed to a positive phase of the AMO (Sun et al., 2020).

The AMO was persistent across the Holocene with a 55–80 years cycle, and it is highly associated with the multidecadal variability of the Atlantic meridional overturning circulation (Knudsen et al., 2011; Wei and Lohmann, 2012). During the early Holocene, the intertropical convergence zone shifted northward (Jin et al., 2014; Zhang and Jin, 2018), the ISM substantially intensified (Fleitmann et al., 2007; Bird et al., 2014), the north hemisphere subtropical westerly jet shifted northward (**Figure 13B**), and the AMO was in a positive state (**Figure 13C**). Together these driving forces induced a wave train of cyclonic and anticyclonic anomalies during the growing season,

enhancing the meandering of the westerly jet (Mölg et al., 2017; Sun et al., 2020). Due to this enhancement, the cyclonic circulation on the west side of TP enhanced that further caused southwesterly winds on the southwestern flank of the TP intensified, but westerly winds over the TP weakened as the subtropical westerly jet shifted northward. As with modern precipitation shifts, this "up-and-over" moisture transport pattern resulted in a substantial increase in precipitation in the southwestern ITP since water vapor crossing the high mountains initially arrives in that part of the ITP, producing more rainfall than further to the north and northeast (Liu et al., 2019).

Since the early mid-Holocene, the northern hemisphere subtropical westerly jet shifted southward (**Figure 13B**), and the AMO became increasingly negative between 8 and 6 ka, before rising slightly again during the past 2 ka (**Figure 13C**). As the position of the westerly jet shifted southward and the AMO changed to a negative phase, the ISM also weakened after the mid-Holocene. Water vapor introduced into the ITP was reduced, but water vapor transport across its east boundary increased, causing lakes in the ITP to shrink in response to a net loss of precipitation.

It is noteworthy that while increased precipitation over the western ITP was not as great as in the southwestern ITP during the early Holocene (**Figure 10A**), lakes in this area also expanded markedly (**Figure 8**). It has been suggested that glacier melt water from an ice cap in the western TP was at maximum during the early Holocene (Li et al., 2021), and as a result we propose that lakes in western ITP may have expanded due to increased glacier melt water supply as well as to increased rainfall related to the intensified ISM.

## CONCLUSION

In this study we investigate Holocene lake level variations in ITP and their driving forces by combining reported lake level variation curves and spatial lake expansion patterns, with TraCE-21ka and KCM simulated precipitation and P-E changes over the ITP. We draw the following conclusions: 1) The highest lake levels appeared during the early Holocene (10–8 ka), and lake levels started to decline after the mid-Holocene. 2) This early Holocene expansion was greatest in the southwestern and western ITP, but the magnitude of lake transgressions decreased toward the northern and northeastern ITP. 3) TraCE-21ka and KCM simulation results show that a summer and autumn precipitation increase may be the main reason for Holocene lake expansions in the southern, central, and northern ITP, while increased glacier melt water accompanied by an increase in summer rainfall caused lakes in the western ITP to dramatically expand. 4) During the early Holocene the ISM intensified in response to a northward shift of the tropical convergence zone, with the northern hemisphere westerly jet also shifting northward and with the AMO in a positive phase. As a result, southwesterly winds on the southwestern flank of the TP were enhanced, while westerly winds over the TP decreased, causing more water vapor to be transported to the ITP through the "up-and-over" moisture transport route and stuck in there. The amount of enhanced precipitation decreased from the southwestern to northeastern ITP, causing lakes in the southwestern ITP to expand to higher levels than those in the central, northern, and northeastern ITP.

## DATA AVAILABILITY STATEMENT

The original contributions presented in the study are included in the article/**Supplementary Material**, further inquiries can be directed to the corresponding author.

## AUTHOR CONTRIBUTIONS

LX designed the research. LX and MD wrote the manuscript. ZX performed the KCM climate modelling.

## FUNDING

This work was funded by the Second TP Scientific Expedition and Research Program (2019QZKK0202) and the National Natural Science Foundation of China (41671006).

## ACKNOWLEDGMENTS

We thank Professor Chen Fahu for help LX joins the Second Tibetan Plateau Scientific Expedition and Research Program. Thanks Professor Yang Kun for his shares of the figure we used in **Figure 13**. We also thank three reviewers for their constructive comments that help improve the quality of this paper. The TraCE-21ka model simulation data were downloaded from http://202.195.239.65:8888/.

## SUPPLEMENTARY MATERIAL

The Supplementary Material for this article can be found online at: https://www.frontiersin.org/articles/10.3389/feart.2021.685928/full#supplementary-material

## REFERENCES

Ahlborn, M., Haberzettl, T., Wang, J., Fürstenberg, S., Mäusbacher, R., Mazzocco, J., et al. (2015). Holocene lake Level History of the Tangra Yumco lake System, Southern-central Tibetan Plateau. *The Holocene* 26, 176–187. doi:10.1177/0959683615596840

Alivernini, M., Lai, Z., Frenzel, P., Fürstenberg, S., Wang, J., Guo, Y., et al. (2018). Late Quaternary lake Level Changes of Taro Co and Neighbouring Lakes, Southwestern Tibetan Plateau, Based on OSL Dating and Ostracod

Analysis. *Glob. Planet. Change* 166, 1–18. doi:10.1016/j.gloplacha.2018.03.016

Barnett, T. P., Adam, J. C., and Lettenmaier, D. P. (2005). Potential Impacts of a Warming Climate on Water Availability in Snow-Dominated Regions. *Nature* 438, 303–309. doi:10.1038/nature04141

Bird, B. W., Polisar, P. J., Lei, Y., Thompson, L. G., Yao, T., Finney, B. P., et al. (2014). A Tibetan lake Sediment Record of Holocene Indian Summer Monsoon Variability. *Earth Planet. Sci. Lett.* 399, 92–102. doi:10.1016/j.epsl.2014.05.017

Cai, Y., Zhang, H., Cheng, H., An, Z., Lawrence Edwards, R., Wang, X., et al. (2012). The Holocene Indian Monsoon Variability over the Southern Tibetan Plateau and its Teleconnections. *Earth Planet. Sci. Lett.* 335-336, 135–144. doi:10.1016/j.epsl.2012.04.035

Chen, F., Zhang, J., Liu, J., Cao, X., Hou, J., Zhu, L., et al. (2020). Climate Change, Vegetation History, and Landscape Responses on the Tibetan Plateau during the Holocene: a Comprehensive Review. *Quat. Sci. Rev.* 243, 106444. doi:10.1016/j.quascirev.2020.106444

Chen, Y., Zong, Y., Li, B., Li, S., and Aitchison, J. C. (2013). Shrinking Lakes in Tibet Linked to the Weakening Asian Monsoon in the Past 8.2 Ka. *Quat. Res.* 80, 189–198. doi:10.1016/j.yqres.2013.06.008

Cheng, J., Wu, H., Liu, Z., Gu, P., Wang, J., Zhao, C., et al. (2021). Vegetation Feedback Causes Delayed Ecosystem Response to East Asian Summer Monsoon Rainfall during the Holocene. *Nat. Commun.* 12, 1843. doi:10.1038/s41467-021-22087-2

Conroy, J. L., and Overpeck, J. T. (2011). Regionalization of Present-Day Precipitation in the Greater Monsoon Region of Asia*. *J. Clim.* 24, 4073–4095. doi:10.1175/2011JCLI4033.1

Dai, Y., Chen, D., Yao, T., and Wang, L. (2020b). Large Lakes over the Tibetan Plateau May Boost Snow Downwind: Implications for Snow Disaster. *Sci. Bull.* 65, 1713–1717. doi:10.1016/j.scib.2020.06.012

Dai, Y., Yao, T., Wang, L., Li, X., and Zhang, X. (2020a). Contrasting Roles of a Large Alpine Lake on Tibetan Plateau in Shaping Regional Precipitation during Summer and Autumn. *Front. Earth Sci.* 8, 358. doi:10.3389/feart.2020.00358

Dong, W., Lin, Y., Wright, J. S., Ming, Y., Xie, Y., Wang, B., et al. (2016). Summer Rainfall over the Southwestern Tibetan Plateau Controlled by Deep Convection Over the Indian Subcontinent. *Nat. Commun.* 7, 10925. doi:10.1038/ncomms10925

Fleitmann, D., Burns, S. J., Mangini, A., Mudelsee, M., Kramers, J., Villa, I., et al. (2007). Holocene ITCZ and Indian Monsoon Dynamics Recorded in Stalagmites from Oman and Yemen (Socotra). *Quat. Sci. Rev.* 26, 170–188. doi:10.1016/j.quascirev.2006.04.012

Gasse, F., Arnold, M., Fontes, J.C., Gibert, E., Fort, M., Huc, A., et al. (1991). A 13000-year climate record from western Tibet. *Nature* 353, 742–745.

Herzschuh, U., Cao, X., Laepple, T., Dallmeyer, A., Telford, R. J., Ni, J., et al. (2019). Position and Orientation of the westerly Jet Determined Holocene Rainfall Patterns in China. *Nat. Commun.* 10, 2376. doi:10.1038/s41467-019-09866-8

Hou, S. (2019). How Old Are the Tibetan Ice Cores? *Chin. Sci. Bull.* 64, 2425–2429. [in Chinese]. doi:10.1360/N972019-00189

Hou, Y., Long, H., Gao, L., and Shen, J. (2020). Luminescence Dating of Lacustrine Sediments from CuoE lake on the central Tibetan Plateau. *Geochronometria*. in press. doi:10.2478/geochr-2020-0002

Hou, Y., Long, H., Shen, J., and Gao, L. (2021). Holocene lake-level Fluctuations of Selin Co on the central Tibetan Plateau: Regulated by Monsoonal Precipitation or Meltwater? *Quat. Sci. Rev.* 261, 106919. doi:10.1016/j.quascirev.2021.106919

Hudson, A. M., Quade, J., Huth, T. E., Lei, G., Cheng, H., Edwards, L. R., et al. (2015). Lake Level Reconstruction for 12.8-2.3 Ka of the Ngangla Ring Tso Closed-Basin Lake System, Southwest Tibetan Plateau. *Quat. Res.* 83, 66–79. doi:10.1016/j.yqres.2014.07.012

Hudson, A. M., and Quade, J. (2013). Long-term East-West Asymmetry in Monsoon Rainfall on the Tibetan Plateau. *Geology* 41, 351–354. doi:10.1130/G33837.1

Huth, T., Hudson, A. M., Quade, J., Guoliang, L., and Hucai, Z. (2015). Constraints on Paleoclimate from 11.5 to 5.0 Ka from Shoreline Dating and Hydrologic Budget Modeling of Baqan Tso, Southwestern Tibetan Plateau. *Quat. Res.* 83, 80–93. doi:10.1016/j.yqres.2014.07.011

Immerzeel, W. W., van Beek, L. P. H., and Bierkens, M. F. P. (2010). Climate Change Will Affect the Asian Water Towers. *Science* 328, 1382–1385. doi:10.1126/science.1183188

Jin, L., Schneider, B., Park, W., Latif, M., Khon, V., and Zhang, X. (2014). The Spatial-Temporal Patterns of Asian Summer Monsoon Precipitation in Response to Holocene Insolation Change: a Model-Data Synthesis. *Quat. Sci. Rev.* 85, 47–62. doi:10.1016/j.quascirev.2013.11.004

Jonell, T. N., Aitchison, J. C., Li, G., Shulmeister, J., Zhou, R., and Zhang, H. (2020). Revisiting Growth and Decline of Late Quaternary Mega-Lakes across the South-central Tibetan Plateau. *Quat. Sci. Rev.* 248, 106475. doi:10.1016/j.quascirev.2020.106475

Knudsen, M. F., Seidenkrantz, M.-S., Jacobsen, B. H., and Kuijpers, A. (2011). Tracking the Atlantic Multidecadal Oscillation through the Last 8,000 Years. *Nat. Commun.* 2, 178. doi:10.1038/ncomms1186

Lai, H.-W., Chen, H. W., Kukulies, J., Ou, T., and Chen, D. (2021). Regionalization of Seasonal Precipitation over the Tibetan Plateau and Associated Large-Scale Atmospheric Systems. *J. Clim.* 34, 2635–2651. doi:10.1175/JCLI-D-20-0521.1

Lee, J., Li, S.-H., and Aitchison, J. C. (2009). OSL Dating of Paleoshorelines at Lagkor Tso, Western Tibet. *Quat. Geochronol.* 4, 335–343. doi:10.1177/095968361140523210.1016/j.quageo.2009.02.003

Lei, Y., Yang, K., Wang, B., Sheng, Y., Bird, B. W., Zhang, G., et al. (2014). Response of Inland lake Dynamics over the Tibetan Plateau to Climate Change. *Climatic Change* 125, 281–290. doi:10.1007/s10584-014-1175-3

Li, C.-G., Wang, M., Liu, W., Lee, S.-Y., Chen, F., and Hou, J. (2021). Quantitative Estimates of Holocene Glacier Meltwater Variations on the Western Tibetan Plateau. *Earth Planet. Sci. Lett.* 559, 116766. doi:10.1016/j.epsl.2021.116766

Li, D., Li, Y., Ma, B., Dong, G., Wang, L., and Zhao, J. (2009). Lake-level Fluctuations since the Last Glaciation in Selin Co (lake), Central Tibet, Investigated Using Optically Stimulated Luminescence Dating of beach Ridges. *Environ. Res. Lett.* 4, 045204. doi:10.1088/1748-9326/4/4/045204

Li, G., Xue, S., Yao, Z., and Gao, S. (1992). Evaporation of Brine at Different Concentrations in the Sun Farm Area of Lake Da-Qaidam. *Saltlake salt Chem. industry* 2, 13–17. [in Chinese].

Li, Y., Su, F., Chen, D., and Tang, Q. (2019). Atmospheric Water Transport to the Endorheic Tibetan Plateau and its Effect on the Hydrological Status in the Region. *J. Geophys. Res. Atmos.* 124, 12864–12881. doi:10.1029/2019JD031297

Liu, B., Du, Y. e., Li, L., Feng, Q., Xie, H., Liang, T., et al. (2016a). Outburst Flooding of the Moraine-Dammed Zhuonai Lake on Tibetan Plateau: Causes and Impacts. *IEEE Geosci. Remote Sensing Lett.Remote Sens. Lett.* 13, 570–574. doi:10.1109/LGRS.2016.2525778

Liu, X.-J., Lai, Z.-P., Zeng, F.-M., Madsen, D. B., and E, C.-Y. (2013). Holocene lake Level Variations on the Qinghai-Tibetan Plateau. *Int. J. Earth Sci. (Geol Rundsch)* 102, 2007–2016. doi:10.1007/s00531-013-0896-2

Liu, X.-J., Madsen, D. B., Liu, R., Sun, Y., and Wang, Y. (2016b). Holocene lake Level Variations of Longmu Co, Western Qinghai-Tibetan Plateau. *Environ. Earth Sci.* 75, 301. doi:10.1007/s12665-015-5188-7

Liu, X., Cong, L., Li, X., Madsen, D., Wang, Y., Liu, Y., et al. (2020). Climate Conditions on the Tibetan Plateau during the Last Glacial Maximum and Implications for the Survival of Paleolithic Foragers. *Front. Earth Sci.* 8, 606051. doi:10.3389/feart.2020.606051

Liu, X., Zhang, X., Lin, Y., Jin, L., and Chen, F. (2019). Strengthened Indian Summer Monsoon Brought More Rainfall to the Western Tibetan Plateau during the Early Holocene. *Sci. Bull.* 64, 1482–1485. doi:10.1016/j.scib.2019.07.022

Liu, Y., Chen, H., Li, H., Zhang, G., and Wang, H. (2021). What Induces the Interdecadal Shift of the Dipole Patterns of Summer Precipitation Trends over the Tibetan Plateau? *Int. J. Climatol.*, 1–19. doi:10.1002/joc.7122

Liu, Z., Otto-Bliesner, B. L., He, F., Brady, E. C., Tomas, R., Clark, P. U., et al. (2009). Transient Simulation of Last Deglaciation with a New Mechanism for Bolling-Allerod Warming. *Science* 325, 310–314. doi:10.1126/science.1171041

Long, H., Lai, Z., Frenzel, P., Fuchs, M., and Haberzettl, T. (2012). Holocene Moist Period Recorded by the Chronostratigraphy of a lake Sedimentary Sequence from Lake Tangra Yumco on the South Tibetan Plateau. *Quat. Geochronol.* 10, 136–142. doi:10.1016/j.quageo.2011.11.005

Ma, N., Ma, Z., Zheng, M., and Wang, H. (2012). 230Th Dating of Stem Carbonate Deposits from Tai Cuo lake, Western Tibetan Plateau, China. *Quat. Int.* 250, 55–62. doi:10.1016/j.quaint.2011.09.012

Mölg, T., Maussion, F., Collier, E., Chiang, J. C. H., and Scherer, D. (2017). Prominent Midlatitude Circulation Signature in High Asia's Surface Climate

during Monsoon. *J. Geophys. Res. Atmos.* 122, 12702–12712. doi:10.1002/2017JD027414

Pan, B., Yi, C., Jiang, T., Dong, G., Hu, G., and Jin, Y. (2012). Holocene lake-level Changes of Linggo Co in central Tibet. *Quat. Geochronol.* 10, 117–122. doi:10.1016/j.quageo.2012.03.009

Park, W., Keenlyside, N., Latif, M., Ströh, A., Redler, R., Roeckner, E., et al. (2009). Tropical Pacific Climate and its Response to Global Warming in the Kiel Climate Model. *J. Clim.* 22, 71–92. doi:10.1175/2008JCLI2261.1

Qiao, B., Zhu, L., and Yang, R. (2019). Temporal-spatial Differences in lake Water Storage Changes and Their Links to Climate Change throughout the Tibetan Plateau. *Remote Sensing Environ.* 222, 232–243. doi:10.1016/j.rse.2018.12.037

Quade, J., and Broecker, W. S. (2009). Dryland Hydrology in a Warmer World: Lessons From the Last Glacial Period. *Eur. Phys. J. Spec. Top.* 176, 21–36. doi:10.1140/epjst/e2009-01146-y

Rades, E. F., Hetzel, R., Xu, Q., and Ding, L. (2013). Constraining Holocene lake-level Highstands on the Tibetan Plateau by 10Be Exposure Dating: a Case Study at Tangra Yumco, Southern Tibet. *Quat. Sci. Rev.* 82, 68–77. doi:10.1016/j.quascirev.2013.09.016

Shi, X., Kirby, E., Furlong, K. P., Meng, K., Robinson, R., Lu, H., et al. (2017). Rapid and Punctuated Late Holocene Recession of Siling Co, central Tibet. *Quat. Sci. Rev.* 172, 15–31. doi:10.1016/j.quascirev.2017.07.017

Sun, J., Yang, K., Guo, W., Wang, Y., He, J., and Lu, H. (2020). Why Has the Inner Tibetan Plateau Become Wetter since the Mid-1990s? *J. Clim.* 33, 8507–8522. doi:10.1175/JCLI-D-19-0471.1

Wei, W., and Lohmann, G. (2012). Simulated Atlantic Multidecadal Oscillation during the Holocene. *J. Clim.* 25, 6989–7002. doi:10.1175/JCLI-D-11-00667.1

Yan, Q., Owen, L. A., Wang, H., and Zhang, Z. (2018). Climate Constraints on Glaciation over High-Mountain Asia during the Last Glacial Maximum. *Geophys. Res. Lett.* 45, 9024–9033. doi:10.1029/2018GL079168

Yan, Q., Owen, L. A., Zhang, Z., Jiang, N., and Zhang, R. (2020). Deciphering the Evolution and Forcing Mechanisms of Glaciation over the Himalayan-Tibetan Orogen during the Past 20,000 Years. *Earth Planet. Sci. Lett.* 541, 116295. doi:10.1016/j.epsl.2020.116295

Yang, K., Lu, H., Yue, S., Zhang, G., Lei, Y., La, Z., et al. (2018). Quantifying Recent Precipitation Change and Predicting lake Expansion in the Inner Tibetan Plateau. *Climatic Change* 147, 149–163. doi:10.1007/s10584-017-2127-5

Yao, T., Thompson, L., Yang, W., Yu, W., Gao, Y., Guo, X., et al. (2012). Different Glacier Status with Atmospheric Circulations in Tibetan Plateau and Surroundings. *Nat. Clim Change* 2, 663–667. doi:10.1038/nclimate1580

Yao, X., Sun, M., Gong, P., Liu, B., Li, X., An, L., et al. (2016). Overflow Probability of the Salt Lake in Hoh Xil Region. *Acta Geographica Sinica* 71 (9), 1520–1527. [in Chinese, with English Abstract]. doi:10.11821/dlxb201609005

Zhang, C., Tang, Q., Chen, D., Van Der Ent, R. J., Liu, X., Li, W., et al. (2019b). Moisture Source Changes Contributed to Different Precipitation Changes over the Northern and Southern Tibetan Plateau. *J. Hydrometeorol.* 20, 217–229. doi:10.1175/JHM-D-18-0094.1

Zhang, G., Chen, W., and Xie, H. (2019a). Tibetan Plateau's Lake Level and Volume Changes from NASA's ICESat/ICESat-2 and Landsat Missions. *Geophys. Res. Lett.* 46 (13), 13107–13118. doi:10.1029/2019GL085032

Zhang, G., Yao, T., Xie, H., Kang, S., and Lei, Y. (2013). Increased Mass over the Tibetan Plateau: From Lakes or Glaciers? *Geophys. Res. Lett.* 40, 2125–2130. doi:10.1002/grl.50462

Zhang, G., Yao, T., Xie, H., Yang, K., Zhu, L., Shum, C. K., et al. (2020). Response of Tibetan Plateau Lakes to Climate Change: Trends, Patterns, and Mechanisms. *Earth-Science Rev.* 208, 103269. doi:10.1016/j.earscirev.2020.103269

Zhang, X., Jin, L., and Jia, W. (2016). Centennial-scale Teleconnection between North Atlantic Sea Surface Temperatures and the Indian Summer Monsoon during the Holocene. *Clim. Dyn.* 46, 3323–3336. doi:10.1007/s00382-015-2771-2

Zhang, X., and Jin, L. (2018). Meridional Migration of the South Asian High and its Association With Asian Summer Monsoon Precipitation during the Holocene. *Quat. Sci.* 38, 1244–1254. [in Chinese, with English Abstract]. doi:10.11928/j.issn.1001-7410.2018.05.18

Zhang, Y., Zhang, J., McGowan, S., Metcalfe, S., Jones, M., Leng, M. J. M., et al. (2021). Climatic and Environmental Change in the Western Tibetan Plateau during the Holocene, Recorded by lake Sediments from Aweng Co. *Quat. Sci. Rev.* 259, 106889. doi:10.1016/j.quascirev.2021.106889

Zhao, K., Zhou, X., Ji, M., and Li, X. (2019). Palynological Evidence of Late Holocene Paleo-Monsoon in Eastern Pamir. *Geophys. Res. Lett.* 46, 10015–10023. doi:10.1029/2019GL082941

Zhao, Y., and Zhou, T. (2021). Interannual Variability of Precipitation Recycle Ratio over the Tibetan Plateau. *J. Geophys. Res.-Atmos.* 126, e2020JD033733. doi:10.1029/2020jd033733

Zhu, L., Lü, X., Wang, J., Peng, P., Kasper, T., Daut, G., et al. (2015). Climate Change on the Tibetan Plateau in Response to Shifting Atmospheric Circulation since the LGM. *Sci. Rep.* 5, 13318. doi:10.1038/srep13318

**Conflict of Interest:** The authors declare that the research was conducted in the absence of any commercial or financial relationships that could be construed as a potential conflict of interest.